39th AIAA/ASME/SAE/ASEE
Joint Propulsion Conference and Exhibit
July 20-23, 2003, Huntsville, AL

Paper 2003-4822

THE EFFECT OF A POROUS THRUST SURFACE ON DETONATION TUBE IMPULSE

M. Cooper, J. Jewell and J.E. Shepherd
Graduate Aeronautical Laboratories,
California Institute of Technology, Pasadena, CA 91125

As pulse detonation engine (PDE) development matures, it becomes increasingly important to consider how practical details such as the implementation of valves and nozzles will affect performance. Inlet valve timing and valveless inlet designs may result in flow of products back upstream and, consequently, reduction in impulse over the ideal case. While proper inlet design or operation under flowing conditions may minimize these losses, our study addresses the worst-case effect that a porous thrust surface may have on the measured impulse. A series of single-cycle tests have been carried out to measure the impulse in a detonation tube with a porous thrust surface. The impulse was measured for porous thrust surfaces with blockage ratios ranging from completely solid (100% blockage ratio) to completely open (0% blockage ratio) at initial pressures from 20 to 100 kPa in stoichiometric ethylene-oxygen mixtures ignited with a weak spark. All tests were conducted at an ambient pressure of 100 kPa. A 76% loss in impulse was observed with a thrust surface blockage ratio of 52% at an initial pressure of 100 kPa. The time to detonation transition was found to be more dependent on the initial pressure of the combustible mixture than on the thrust surface blockage ratio. A model of the impulse in detonation tubes with porous thrust surfaces was developed which reliably predicts the experimental trends.

Nomenclature

A	cross-sectional area
A^*	cross-sectional area at sonic conditions
A_f	free area of holes in thrust surface
BR	blockage ratio
c^*	sound speed at sonic conditions
c_2	detonation wave sound speed
c_3	sound speed in products after passage of Taylor wave for a solid thrust surface
$c_{3'}$	sound speed in products after passage of Taylor wave for a porous thrust surface
D	detonation tube diameter
F	x-direction force acting on the control volume
f	friction factor
g	standard gravitational acceleration
I	single-cycle impulse with solid thrust surface
I'	single-cycle impulse with porous thrust surface
I_{SP}	mixture-based specific impulse
I_V	impulse per unit volume
K	proportionality constant
L	detonation tube length
L_p	length of pendulum arm
m	detonation tube mass
M_2	detonation wave Mach number
M_3	Mach number after passage of Taylor wave with a solid thrust surface
$M_{3'}$	Mach number after passage of Taylor wave with a porous thrust surface
p	thrust surface porosity
$P(t)$	time varying pressure acting on the internal face of the thrust surface
P^*	critical pressure
P_0	environment pressure
P_1	pressure of reactants
P_3	pressure after passage of Taylor wave with a solid thrust surface
$P_{3'}$	pressure after passage of Taylor wave with a porous thrust surface
P_{CJ}	Chapman-Jouguet detonation pressure
t	time
t_1	time taken by the detonation wave to reach the open end of the tube
t_2	time taken by the first reflected characteristic to reach the thrust surface

U_{CJ}	Chapman-Jouguet detonation speed
u	velocity
u_2	lab frame velocity at sonic plane behind detonation wave
u_3	velocity after passage of Taylor wave for a solid thrust surface
$u_{3'}$	velocity after passage of Taylor wave for a porous thrust surface
V	inner volume of detonation tube
x	distance
Δx	horizontal displacement of pendulum
γ	ratio of specific heats of detonation products
ρ	density
ρ^*	density at sonic conditions
ρ_1	density of reactants
ρ_3	density of products after passage of Taylor wave with a solid thrust surface
$\rho_{3'}$	density of products after passage of Taylor wave with a porous thrust surface
τ	wall shear stress

Introduction

As pulse detonation engine (PDE) development progresses, increasing attention is being placed on inlet valves and other upstream flow features. Previous single-cycle experimental studies[1–7] have been conducted with simplified detonation tube geometries and have quantified the impulse obtained from a variety of combustible mixtures at varying initial pressures and dilution amounts in addition to investigating the effect of internal obstacles,[1,2] deflagration to detonation transition (DDT) distance,[1,3] and attached nozzles[1,4–7] on impulse.

In these experiments, however, the detonation tube thrust surface was solid (100% blockage ratio) and all exhaust flow was forced to exit through the open end of the tube. In a practical multi-cycle application, the thrust surface of the tube will not be solid since a fresh combustible mixture must be repeatedly injected. A variety of inlet designs[4,8–11] and mechanical valves have already been implemented into multi-cycle test facilities.

Because of the many variations in inlet design, the actual loss in impulse must be determined on an individual basis. It is possible with proper inlet design that the impulse may not be transferred to a thrust surface in the typical sense but to another part of the engine. Valveless PDE's that operate under flowing conditions in which the upstream flow is choked could be thought of as a 'fluidic' thrust surface where losses in impulse are minimized. Non-optimum inlet design may significantly affect the measured impulse even for relatively small values of thrust surface porosity. Improper valve timing could result in open valves while the detonation is propagating the length of the tube resulting in product gas exhaust out through the inlet valves. To study this aspect of PDE performance, we have selected the simplest possible geometry which will show this effect. This study is conducted in a non-flowing, single-cycle detonation tube that is closed by a porous plate at the thrust end and open at the opposite end. We used the ballistic pendulum technique to experimentally determine the impulse and have developed a simple model to predict the impulse given the thrust surface blockage ratio. The impulse results obtained are considered to be the worst-case and can be used to bound any losses in impulse that may occur due to the physical dimensions of a PDE inlet.

Experimental setup

Tests were conducted in a detonation tube of constant cylindrical cross-section (Fig. 1). The tube had an inner diameter of 76.2 mm, a length of 1.057 m, and did not contain internal obstacles. A porous (or solid) thrust surface was installed at one end of the tube near the spark plug and sealed with a 25 μm thick Mylar diaphragm. A fixture was built enabling different thrust surfaces to be easily exchanged. The exhaust end was open but initially sealed with a second 25 μm thick Mylar diaphragm. Direct impulse measurements were made by hanging the tube from the ceiling in a ballistic pendulum arrangement with four steel wires. The tube's maximum horizontal deflection Δx was recorded and used to calculate the impulse.

$$I = m\sqrt{2gL_p\left(1-\sqrt{1-\left(\frac{\Delta x}{L_p}\right)^2}\right)} \qquad (1)$$

The experimental uncertainty associated with the single-cycle impulse measured in this fashion was estimated to be $\pm 6.4\%$ for cases of fast DDT.[1]

A spark plug and associated discharge system with 30 mJ of stored energy was used to ignite the combustible mixture at a distance of 43.4 mm from the internal edge of the thrust surface. Combustion products were free to exhaust from the tube's open end and through the porous thrust surface into a large ($\simeq$ 50 m^3) blast-proof room. Diagnostics on the detonation tube included four pressure transducers and ten ionization gauges.

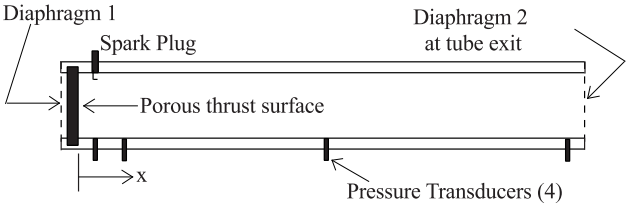

Fig. 1 Schematic of the experimental detonation tube with porous thrust surface.

Each test began by installing a diaphragm at both ends of the tube and evacuating it to a pressure less

than 27 Pa. A 14 L vessel was filled with stoichiometric ethylene-oxygen by the method of partial pressures and mixed for at least five minutes to ensure homogeneity. The detonation tube was then filled with this premixed gas to an initial pressure between 20 and 100 kPa.

Nine different thrust surfaces were tested with varying hole configurations (Fig. 2). Each thrust surface consisted of a 19.1 mm thick aluminum circular plate with an arrangement of through-holes drilled to yield the desired porosity. The thrust surface porosity p

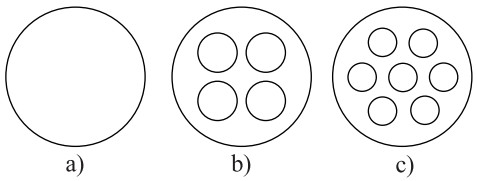

Fig. 2 Porous thrust surfaces with a) solid configuration, b) 4-hole configuration, and c) 7-hole configuration.

is defined as the area of the holes A_f divided by the exposed area of the thrust surface A (equal to the detonation tube cross-sectional area). Alternatively, the blockage ratio (BR) is defined as the blocked area divided by the maximum free area possible on the thrust surface or,

$$BR = 1 - p = 1 - \frac{A_f}{A} \ . \tag{2}$$

Specifics of the experimental thrust surfaces appear in Table 1. The blockage ratios ranged from solid (100% BR) to completely open (0% BR).

Configuration	BR (%)	p (%)
Solid	100	0
4-Hole	88.9	11.1
7-Hole	89.1	10.9
7-Hole	85.1	14.9
7-Hole	80.6	19.4
7-Hole	75.3	24.6
7-Hole	64.9	35.1
7-Hole	52.5	47.5
Open	0	100

Table 1 Blockage ratios and porosities of experimental thrust surfaces.

Impulse modeling

The impulse from a single-cycle detonation tube with a solid thrust surface has been modeled by Wintenberger et al.[12] and is based on a control volume surrounding the detonation tube (Fig. 3). The impulse is obtained by integrating the forces acting on the control volume.

$$I = \int F dt = \int (P(t) - P_0) A dt \tag{3}$$

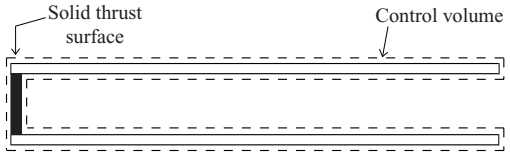

Fig. 3 Control volume for a detonation tube with a solid thrust surface.

Where $P(t)$ is the time-varying pressure acting on the internal face of the thrust surface. This pressure is evaluated by predicting[12] the internal flow field of the detonation tube with one-dimensional gas dynamics assuming instantaneous detonation initiation. A schematic of the thrust surface pressure $P(t)$ appears as the solid line in Fig. 4. Detonation initiation

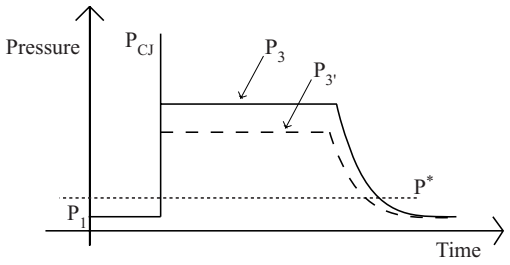

Fig. 4 Thrust surface pressure history for solid and porous thrust surfaces. Solid lines correspond to the case of a solid thrust surface and the dashed lines correspond to the case of a porous thrust surface.

is denoted by the pressure spike to P_{CJ} followed by a region of constant pressure denoted by P_3. This plateau pressure is followed by a region of decreasing pressure as the detonation products exhaust from the tube. The thrust surface pressure history can be integrated exactly to determine the maximum impulse, and the predictions are found to agree within $\pm 15\%$ of experimental data.[12] Alternatively, the results of the exact integration can be approximated by,

$$I = \frac{KV}{U_{CJ}} (P_3 - P_0) \ , \tag{4}$$

which depends on only a few detonation parameters specific to a given initial mixture and can reproduce the predictions of the detailed model to within 2.5%.[12] The volume V represents the product of the tube cross-sectional area A and the tube length L. The proportionality constant K is 4.3. Wintenberger et al.[12] provides a detailed discussion of the model formulation and extensive validation.

Consider now the case of a detonation tube with a porous thrust surface. We modify the previous control volume to account for the open area of the thrust surface (Fig. 5). The impulse is determined by integrating the forces on the control volume in the same manner as above.

$$I' = \int F' dt = \int (P'(t) - P_0) A' dt \tag{5}$$

Fig. 5 Control volume for a detonation tube with a porous thrust surface.

We denote the terms specific to the case with a porous thrust surface with a prime. The instantaneous pressure $P'(t)$ is shown schematically as the dashed line of Fig. 4. The thrust surface area A' represents the thrust surface area that is blocked.

$$A' = A - A_f = A\left(1 - \frac{A_f}{A}\right) \tag{6}$$

Thus, the impulse integral becomes

$$I' = \int (P'(t) - P_0)A\left(1 - \frac{A_f}{A}\right) dt \ . \tag{7}$$

Because of the similarity between the impulse integrals for the cases with a solid and porous thrust surface, we propose a modification to the existing impulse model (Eq. 4) to account for the effect of a porous thrust surface.

$$I' = \frac{KV}{U_{CJ}} (P_{3'} - P_0)\left(1 - \frac{A_f}{A}\right) \tag{8}$$

The volume V still refers to the product of the cross-sectional tube area A and the tube length L. To evaluate the plateau pressure $P_{3'}$ we need to evaluate the internal flow field for a tube with a porous thrust surface.

Internal flow field

When the detonation tube contains a solid thrust surface, the detonation (initiated at or near the thrust surface) propagates the length of the tube followed by an expansion wave called the Taylor wave. This is illustrated by a distance-time diagram in Fig. 6. The

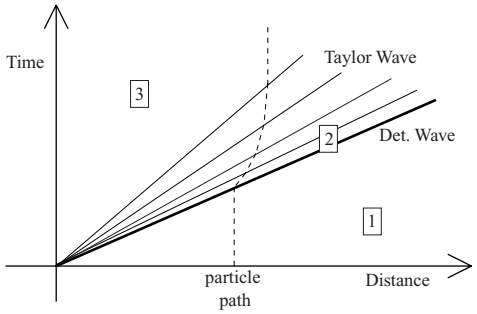

Fig. 6 Distance-time diagram for a detonation tube with a solid thrust surface.

reactant state is labeled on the figures as state 1. State 2 is the Chapman-Jouguet state just behind the detonation wave where the lab frame velocity is u_2 at the sonic plane. Because the flow velocity of a particle next to the solid thrust surface must be zero, the Taylor wave isentropically expands the flow from u_2 at the detonation front to zero at the thrust surface. This is denoted by state 3 where u_3 is zero (Fig. 6). A corresponding pressure decrease occurs through the Taylor wave from the Chapman-Jouguet pressure P_{CJ} to the plateau pressure P_3 (Fig. 4). All detonation products begin to exhaust out the tube exit after the detonation wave transmits a non-reactive shock into the surroundings and a reflected wave back to the thrust surface (not shown in Fig. 6).

When the detonation tube contains a porous thrust surface, the detonation (initiated at or near the thrust surface) travels the length of the tube into the reactive mixture followed by the Taylor wave. However, because of the flow through the thrust surface, some of the detonation products immediately begin to exhaust from the tube resulting in a negative velocity $u_{3'}$ (Fig. 7). To match this non-zero velocity, the Taylor

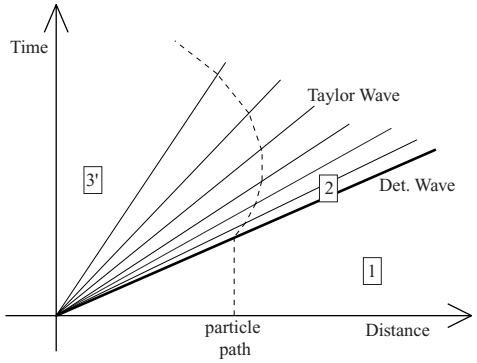

Fig. 7 Distance-time diagram for a detonation tube with a porous thrust surface.

wave must further expand the flow from u_2 to a speed $u_{3'}$ in the direction opposite of the detonation wave propagation. This results in a corresponding plateau pressure $P_{3'}$ at the porous thrust surface that is lower than in the case of a solid thrust surface (Fig. 4).

Because of a decrease in both the plateau pressure and thrust surface area as compared to the case of a solid thrust surface, the impulse is reduced (Eq. 8). As the plateau pressure decreases in response to the decreasing blockage ratio, a corresponding decrease in the impulse is expected. In the limit of a completely open thrust surface (0% BR), the last characteristic of the Taylor wave is sonic at the tube exit and no quasi-steady flow region is established upstream of the thrust surface (Fig. 8). Regardless of the pressure at this location, the predicted impulse is zero since there is no thrust surface area for the pressure differential to act upon.

Calculation of state 3' parameters

To calculate state 3' we assume that a quasi-steady flow with uniform parameters is established behind the Taylor wave. Mass must be conserved so the condition

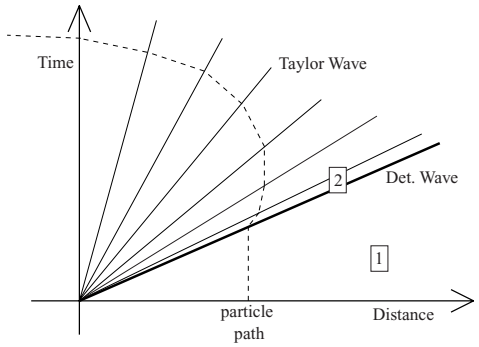

Fig. 8 Distance-time diagram for a detonation tube with a completely open thrust surface. The leftmost C^+ characteristic is sonic and aligned with the y-axis.

that

$$\rho u A(x) = \text{constant} \tag{9}$$

must hold at all locations x within the tube and at the thrust surface. The mass flux ρu is known to be a maximum at the sonic condition. It follows that the area is a minimum at this point and corresponds to the choked area of the thrust surface A^*.

$$\rho^* c^* A^* = \rho_{3'} u_{3'} A \tag{10}$$

The starred terms refer to sonic conditions. By substituting the isentropic relations into Eq. 10, a relation between the choked area and Mach number $M_{3'}$ arises.

$$\frac{A}{A^*} = \frac{1}{M_{3'}} \left(\frac{2}{\gamma+1} + \frac{\gamma-1}{\gamma+1} (M_{3'})^2 \right)^{((\gamma+1)/2(\gamma-1))} \tag{11}$$

We assume an orifice discharge coefficient of one so the choked area A^* in Eq. 11 can be replaced by the physical dimensions of the thrust surface A_f and used to calculate the Mach number $M_{3'}$. The orifice discharge coefficient is known to depend on the Reynolds number for values less than approximately 5000. For larger Reynolds numbers, the discharge coefficient has been measured to be only slightly less than unity.[13,14] Although the cited data on discharge coefficients were generated by studying a single orifice, the results may be extended to the case of a porous plate with regularly spaced holes. For this case, flow losses in perforated plates depend on the blockage ratio, plate thickness to hole diameter ratio, and Reynolds number.[15]

The remaining flow parameters at state 3' are calculated by considering a C^- characteristic through the Taylor wave from the Chapman-Jouguet state.

$$u_2 - \frac{2c_2}{\gamma-1} = u_{3'} - \frac{2c_{3'}}{\gamma-1} \tag{12}$$

The flow velocity at state 2 can be related to the Chapman-Jouguet detonation velocity by the slope of the wave in Fig. 7.

$$\frac{x}{t} = u + c \tag{13}$$

$$\frac{x}{c_2 t} = \frac{u_2 + c_2}{c_2} = \frac{U_{CJ}}{c_2} = M_2 \tag{14}$$

Substituting into Eq. 12 yields,

$$U_{CJ} - c_2 - \frac{2c_2}{\gamma-1} = u_{3'} - \frac{2c_{3'}}{\gamma-1} \ . \tag{15}$$

The ratio of sound speeds across the Taylor wave are determined by manipulating Eq. 15.

$$\frac{c_{3'}}{c_2} = \frac{M_2 - \dfrac{\gamma+1}{\gamma-1}}{M_{3'} - \dfrac{2}{\gamma-1}} \tag{16}$$

The isentropic relations are used to determine the corresponding pressure $P_{3'}$ from the sound speed ratio

$$P_{3'} = P_2 \left(\frac{c_{3'}}{c_2} \right)^{2\gamma/(\gamma-1)} \ . \tag{17}$$

Choked flow assumption

The critical pressure ratio in which sonic flow is established through the thrust surface is a function of the ratio of specific heats γ of the detonation products at state 3'.

$$\frac{P^*}{P_{3'}} = \left(\frac{2}{\gamma+1} \right)^{\dfrac{\gamma}{\gamma-1}} \tag{18}$$

For our experiments, γ is approximately 1.23 in the detonation products which results in a critical pressure ratio of 0.56. If the pressure ratio across the thrust surface $P_0/P_{3'}$ is less than this value, sonic conditions will exist at the thrust surface (Fig. 4). Since the back pressure P_0 on the tube is constant at 0.10 MPa, the thrust surface unchokes when the internal tube pressure reaches 0.18 MPa. After this time, the relationship between area and Mach number of Eq. 11 is no longer valid.

By substituting the calculated $P_{3'}$ into the impulse model, we have assumed the flow through the thrust surface is choked for the entire blowdown process. This causes the impulse to be underpredicted. We estimate the additional loss in impulse due to this assumption by determining the elapsed time during the blowdown process in which the pressure $P'(t)$ is less than the critical pressure and the exhausting flow is expected to be unchoked. From Fig. 9 with a solid thrust surface at an initial pressure of 100 kPa, the blowdown time in which the pressure is between 0.18 MPa and atmospheric pressure is approximately 2 ms. Thus, an additional loss of 8 kg/m^{2}s of impulse is predicted if the pressure is assumed to decrease linearly from 0.18 MPa to 0.10 MPa in 2 ms. This loss is overestimated since

the measured pressure approaches atmospheric pressure faster than linearly. Assuming the impulse model underpredicts the actual impulse by 8 kg/m^{2}s results in an error of less than 1.5% for initial pressures of 100 and 80 kPa, less than 2.5% for an initial pressure of 60 kPa, and less than 4.5% for an initial pressure of 40 kPa at blockage ratios 50% and greater.

Results

Pressure and ionization data

Pressure histories and ionization gauges provide flame acceleration and DDT data. The flame velocity was calculated from the time required for the flame to traverse the distance between two successive ionization gauges. When this velocity was equal to or greater than the Chapman-Jouguet velocity, the flame was said to have transitioned to a detonation. The maximum experimental uncertainty of this transition time is estimated to be ± 43 μs.[1] Figures 9 through 16 plot the pressure histories and ionization data together where pressure and axial distance along the tube are plotted on the y-axis and time along the x-axis. The pressure histories have been offset a distance equal to their axial distance along the tube for clarity. The square data points of the ionization data indicate the time at which the flame or detonation wave has reached the corresponding distance along the tube. The inner thrust wall surface is located at the origin and the tube exit is located at a distance of 1.057 m as denoted on the y-axis (Fig. 1). The first pressure transducer and spark plug are located at a distance of 43.4 mm from the thrust surface. The last pressure transducer and the last ionization gauge are both located 19.0 mm upstream of the tube exit.

In the figures presented below, high frequency oscillations are observed in the pressure histories. They are most apparent in the tests with higher initial pressures (i.e. 100, 80, and 60 kPa). The frequency of these oscillations can be explained by radial pressure oscillations with a period approximately equal to the ratio of the tube diameter to the product sound speed.

Experimental data with a solid thrust surface at different initial pressures is shown in Fig. 9, 10, and 11. In each test, ignition occurs at a time of 3 ms followed by a period of flame acceleration. At 100 kPa initial pressure (Fig. 9), this time period of flame acceleration is the shortest. Transition occurs by the third ionization gauge approximately 0.803 ms after ignition. The pressure histories at the 2nd, 3rd, and 4th gauges show an abrupt overpressure of approximately 4 MPa which is greater than the Chapman-Jouguet pressure of 3.4 MPa, indicating the presence of a detonation. When the initial pressure is reduced to 60 kPa (Fig. 10), the DDT time increases to approximately 1.374 ms. In this case, transition occurs by the 5th ionization gauge. The overpressure spike, although not as large as in the data with 100 kPa initial pressure, does exceed the expected Chapman-Jouguet pressure. As the initial pressure is further reduced to 20 kPa (Fig. 11), the DDT event occurs at the end of the tube. Although the flame velocity as measured by the ionization gauges never exceeds the Chapman-Jouguet detonation speed, an abrupt pressure peak at the 4th pressure gauge is observed. The pressure peak is greater than the Chapman-Jouguet pressure indicating transition does occur in the last 19.0 mm of the tube.

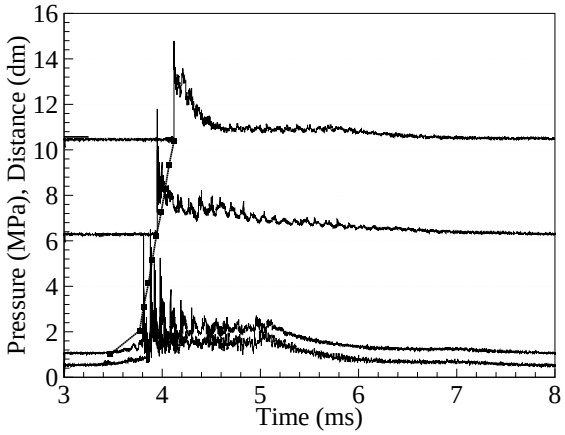

Fig. 9 Shot 209 with a thrust surface blockage ratio of 100% and initial pressure of 100 kPa.

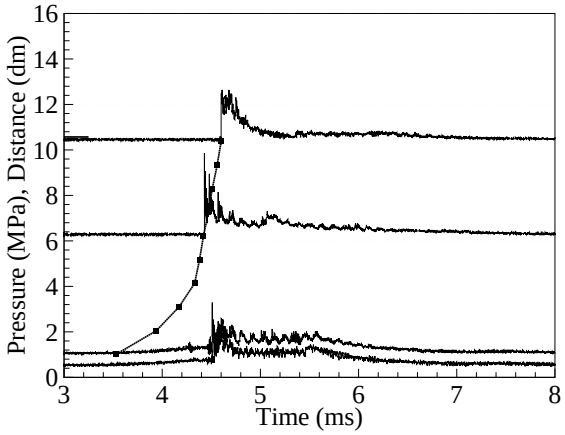

Fig. 10 Shot 207 with a thrust surface blockage ratio of 100% and initial pressure of 59.6 kPa.

Data for a thrust surface blockage ratio of 89.1% and initial pressures of approximately 80 kPa and 40 kPa appear in Fig. 12 and 13, respectively. In these cases, the DDT time increases to approximately 0.547 ms at 80 kPa initial pressure and 0.878 ms at 40 kPa initial pressure. Again, DDT time increases as the initial pressure decreases indicating a decrease in mixture sensitivity. Due to the thrust surface porosity, the arrival of the reflected expansion wave at approximately 5 ms is not as pronounced in the pressure histories as in the case of a solid thrust surface.

Data for an open thrust surface (0% BR) with initial pressure of approximately 100, 60, and 20 kPa

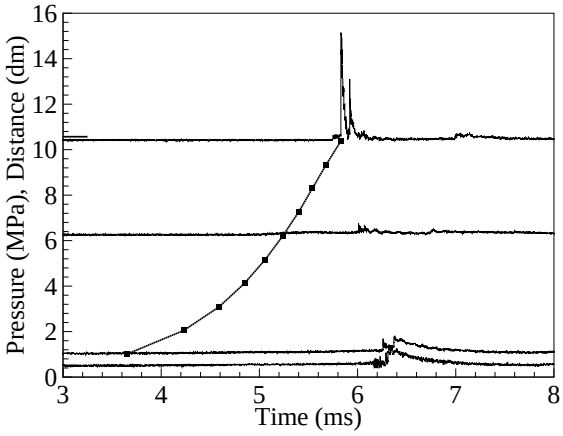

Fig. 11 Shot 206 with a thrust surface blockage ratio of 100% and initial pressure of 20.6 kPa.

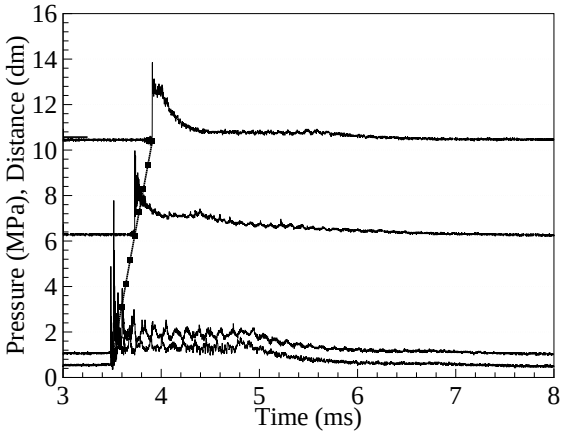

Fig. 12 Shot 203 with a thrust surface blockage ratio of 89.1% and initial pressure of 80.9 kPa.

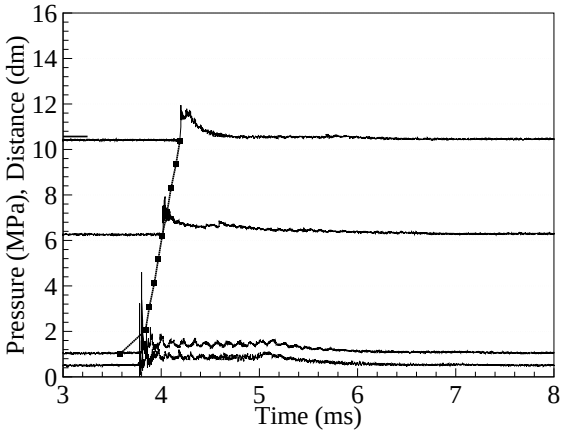

Fig. 13 Shot 202 with a thrust surface blockage ratio of 89.1% and initial pressure of 40.1 kPa.

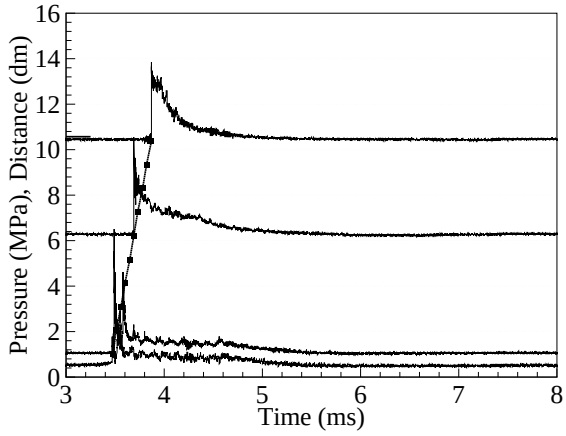

Fig. 14 Shot 237 with a thrust surface blockage ratio of 0% and initial pressure of 100 kPa.

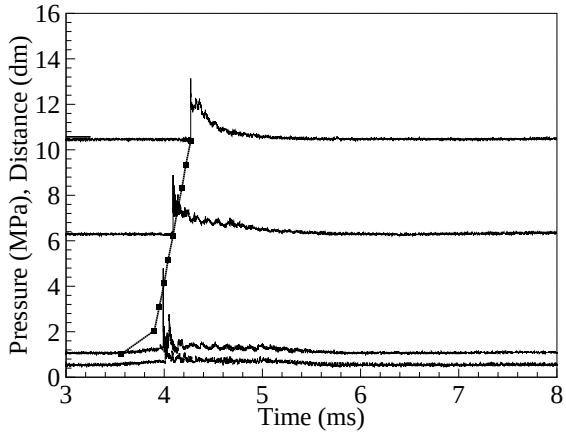

Fig. 15 Shot 235 with a thrust surface blockage ratio of 0% and initial pressure of 58.9 kPa.

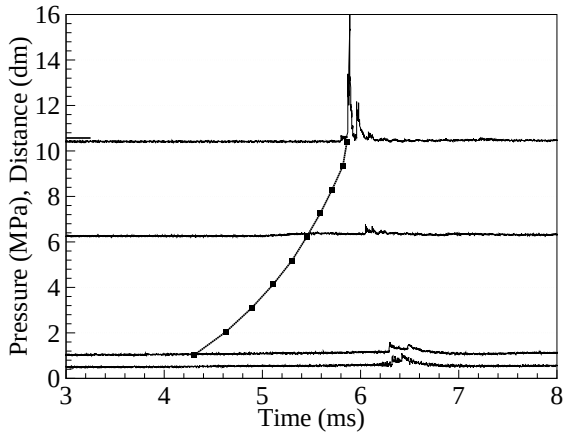

Fig. 16 Shot 236 with a thrust surface blockage ratio of 0% and initial pressure of 20.5 kPa.

appear in Fig. 14, 15, and 16, respectively. DDT time increases with a decrease in pressure. The transition event occurs by the 1st gauge at 100 kPa initial pressure, the 2nd gauge at 60 kPa initial pressure, and the 9th ionization gauge at 20 kPa initial pressure.

Figure 17 further illustrates the effect of decreasing pressure on DDT time. All data points at the different experimental blockage ratios are plotted. The variation in DDT time is at least 1000 μs over the range of initial pressures tested regardless of blockage ratio. This variation is greater than 100% of the average DDT time at a given blockage ratio. Figure 18 plots the same data as a function of blockage ratio. At a given initial pressure, the variation in DDT time

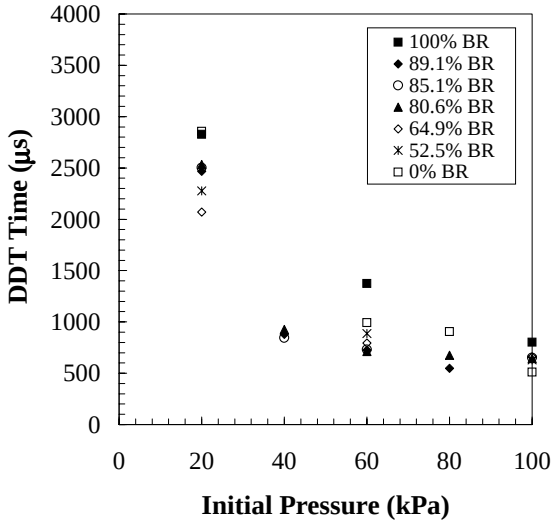

Fig. 17 DDT time as a function of initial pressure.

is no larger than 76% of the average DDT time at a given initial pressure (Table 2). From Fig. 17 and 18,

P_1 (kPa)	Variation in DDT time (μs)	Average DDT time (μs)	Percent (%)
100	293	650	45
80	358	709	50
60	663	873	76
40	83†	883	9
20	786	2467	32

Table 2 Variation and average DDT time over range of tested blockage ratios at each initial pressure. † Only blockage ratios between 89.1% and 80.6% were tested.

the DDT time is more dependent on the mixture's initial pressure than on the thrust surface blockage ratio.

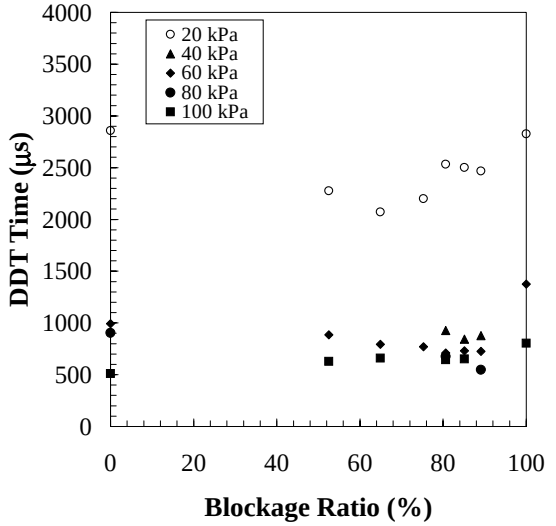

Fig. 18 DDT time as a function of blockage ratio.

Plateau pressure measurements

The calculated values of the thrust surface pressure $P_{3'}$ are compared to the measured values obtained by time averaging the thrust surface pressure history. A subregion of the plateau pressure not affected by pressure oscillations from the passage of the detonation wave or the arrival of the reflected expansion was averaged to obtain a better estimate of the $P_{3'}$ value. Results are plotted as a function of blockage ratio and the predicted values are within ±15% of the experimental values for blockage ratios greater than 0%. The predicted values are an average of 25% less than the experimental values at a blockage ratio of 0%. This difference between the experimental and predicted values at this blockage ratio is likely due to the choked flow assumption of Eq. 11.

The experimental $P_{3'}$ data decreased 27% at an initial pressure of 100 kPa and 19% at an initial pressure of 60 kPa as the blockage ratio decreased to 52.5%.

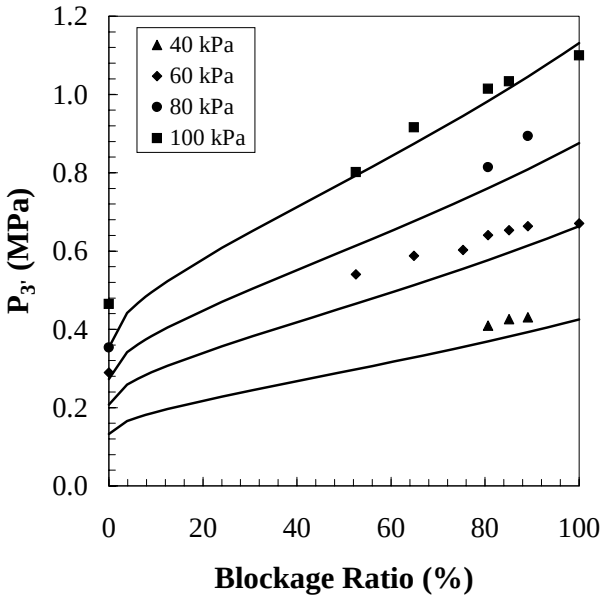

Fig. 19 Plateau pressure $P_{3'}$ versus blockage ratio. The lines correspond to the model predictions of $P_{3'}$ as described by Eqs. 11-17.

Impulse measurements

The experimental data are compared with the model predictions of Eq. 8 as a function of blockage ratio in terms of the impulse per unit volume (Fig. 20) and mixture-based specific impulse (Fig. 21). The impulse per unit volume and specific impulse are related by

$$I_{SP} = \frac{I}{V g \rho_1} = \frac{I_V}{g \rho_1} \ . \qquad (19)$$

Decreasing the blockage ratio to 52.5% results in a 76% decrease in the normalized impulse at an initial pressure of 100 kPa and a 68% decrease in the normalized impulse at an initial pressure of 60 kPa. The model predictions of normalized impulse are within ±13% of

the experimental data for blockage ratios greater than 60%.

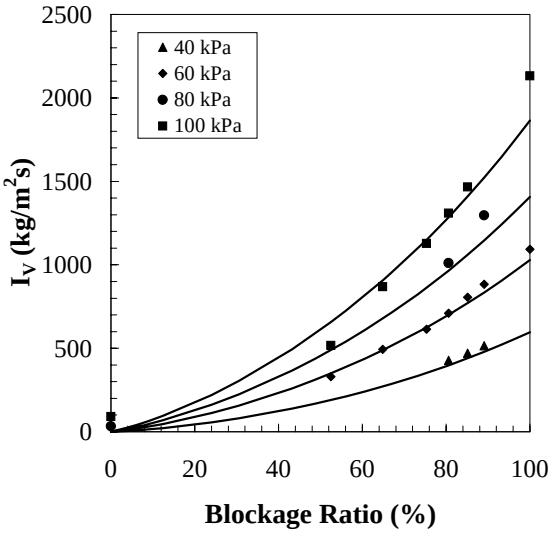

Fig. 20 Impulse measurements as a function of blockage ratio at varying initial pressures. The lines correspond to the model predictions of I_V as described by Eq. 8.

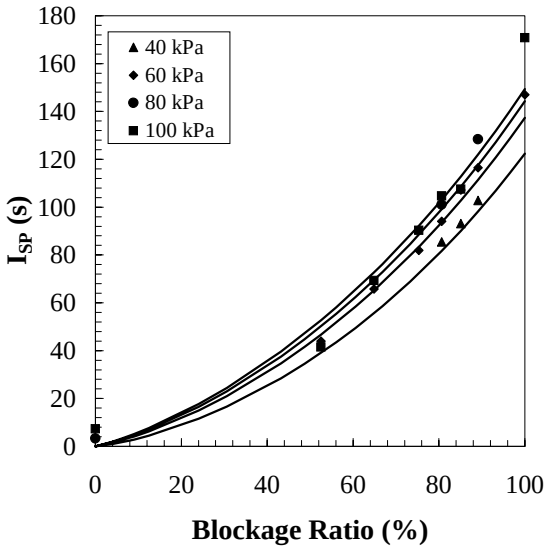

Fig. 21 Specific impulse measurements as a function of blockage ratio for thrust surfaces at varying initial pressures. The lines correspond to the model predictions of I_{SP} as described by Eq. 8 and 19.

Figure 22 plots the experimental impulse values as a function of initial pressure for the different experimental blockage ratios illustrating the increase in impulse with initial pressure.

Experimental impulse data were obtained for a completely open thrust surface (Table 3). At a 0% BR, the model predicts zero impulse since there is no thrust surface for a pressure differential to act upon. However, additional x–direction forces such as wall shear stresses and forces on the wall thickness due to shock

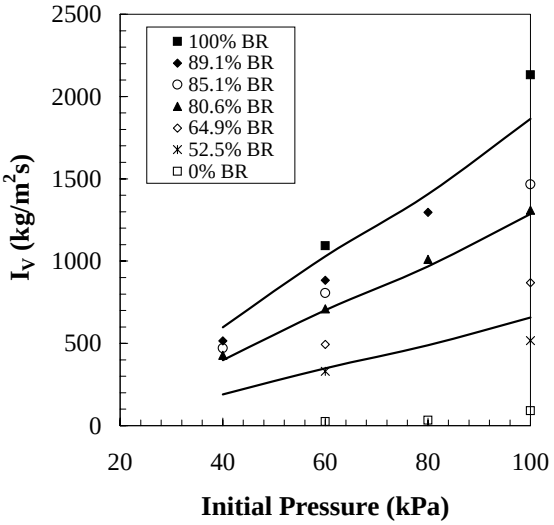

Fig. 22 Impulse measurements as a function of initial pressure for thrust surfaces of varying blockage ratios. Model predictions are plotted as lines for blockage ratios of 100%, 80.6%, and 52.5%.

P_1 (kPa)	I_V (kg/m^{2}s)
100	91.6
80	33.0
60	25.0

Table 3 Estimated and measured normalized impulse for a completely open thrust surface (0% BR).

diffraction outside the tube may act upon the control volume and should be included in the analysis of Eq. 5. We conducted estimates of these additional forces and found that they are likely the cause of the non–zero impulse measured in a completely open tube (Table 3). However, the results were largely inconclusive due to the complexity of the internal flow.

To assess the effect (in any) of the facility on the impulse results, the experimental impulse values for the solid thrust surface are compared with previous experimental data.[1] Over the range of initial pressures tested, the results of this study were within 3% of the previously measured values. The fixture design allowing for easy removal and installation of the different thrust surfaces is most likely the cause of this discrepancy. The solid thrust surfaces did not completely prevent exhaust gases from exiting the tube at the thrust surface end. In fact, the upstream diaphragm was observed to burst entirely during tests at 100 kPa initial pressure, a small hole was observed in the tests at 60 kPa initial pressure, and no disturbance of the diaphragm was observed for the tests at 20 kPa initial pressure. It is expected that the boundary condition of zero velocity at the thrust surface was not strictly met for the tests with higher initial pressure, but this velocity was reasonably small as demonstrated by the agreement with previous impulse data.

As mentioned in the discussion of the tested thrust

surfaces, an additional thrust surface with a 4-hole arrangement was also tested (Fig. 2). This thrust surface had a blockage ratio of 88.9% and was tested at varying initial pressures. A comparison of the impulse between the two thrust surfaces with different hole arrangements and similar blockage ratios illustrates that hole orientation has little effect on the measured impulse (Fig. 23). Instead, the important factor is the area ratio A_f/A. Although only one blockage ratio was tested, this seems to support the work of Kolodzie and Van Winkle who also tested many different hole orientations in their perforated plates and they observed no dependence on hole orientation.[16]

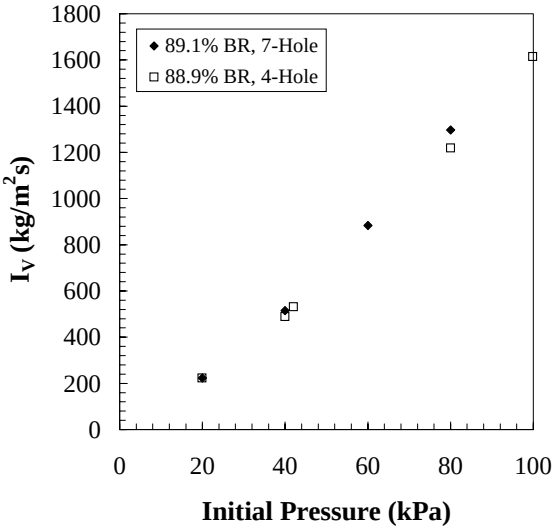

Fig. 23 Impulse measurements as a function of initial pressure for thrust surfaces with similar blockage ratios and different hole configurations.

Conclusion

Single-cycle impulse measurements were obtained with a detonation tube containing a porous thrust surface hung in a ballistic pendulum arrangement. Experiments were completed with blockage ratios between 0% and 100% and initial pressures between 20 and 100 kPa with stoichiometric ethylene-oxygen mixtures. The time required for the initial deflagration to transition to a detonation was found to be more dependent on the initial pressure than on the blockage ratio. The measured impulse was found to decrease as the thrust surface blockage ratio decreased and as the initial pressure decreased. A theoretical model was developed to predict the impulse from a detonation tube with a porous thrust surface and compared to the experimental data. The model assumed the flow exiting the tube through the porous thrust surface was choked and supplied by a region of quasi-steady flow behind the Taylor wave. A method for predicting the thrust surface plateau pressure was discussed. The model is within 15% of the experimental data for blockage ratios greater than 60%.

This research provides information for PDE inlet designers to help predict the maximum losses in impulse that may occur. While specific losses must be evaluated on an individual basis, this research highlights the importance of inlet design. Thus, PDE performance not only depends on the impulse obtained from detonating a specific mixture but also designing the supporting engine components so as to effectively transfer this chemical energy into thrust.

Acknowledgment

This work was supported by the Office of Naval Research Multidisciplinary University Research Initiative *Multidisciplinary Study of Pulse Detonation Engine* (N00014-02-1-0589), and General Electric contract GE-PO A02 81655 under DABT-63-0-0001.

References

[1]Cooper, M., Jackson, S., Austin, J., Wintenberger, E., and Shepherd, J. E., "Direct Experimental Impulse Measurements for Detonations and Deflagrations," *Journal of Propulsion and Power*, Vol. 18, No. 5, 2002, pp. 1033–1041.

[2]Lindstedt, R. P. and Michels, H. J., "Deflagration to Detonation Transitions and Strong Deflagrations in Alkane and Alkene Air Mixtures," *Combust. Flame*, Vol. 76, 1989, pp. 169–181.

[3]Harris, P. G., Farinaccio, R., Stowe, R. A., Higgins, A. J., Thibault, P. A., and Laviolette, J. P., "The Effect of DDT Distance on Impulse in a Detonation Tube," 37th AIAA/ASME/SAE/ASEE Joint Propulsion Conference and Exhibit, July 8–11, 2001, Salt Lake City, UT, AIAA 2001–3467.

[4]Zitoun, R. and Desbordes, D., "Propulsive Performances of Pulsed Detonations," *Comb. Sci. Tech.*, Vol. 144, 1999, pp. 93–114.

[5]Zhdan, S. A., Mitrofanov, V. V., and Sychev, A. I., "Reactive Impulse from the Explosion of a Gas Mixture in a Semi-infinite Space," *Combustion, Explosion and Shock Waves*, Vol. 30, No. 5, 1994, pp. 657–663.

[6]Falempin, F., Bouchaud, D., Forrat, B., Desbordes, D., and Daniau, E., "Pulsed Detonation Engine Possible Application to Low Cost Tactical Missile and to Space Launcher," 37th AIAA/ASME/SAE/ASEE Joint Propulsion Conference and Exhibit, July 8–11, 2001, Salt Lake City, UT, AIAA 2001–3815.

[7]Cooper, M. and Shepherd, J. E., "The Effect of Nozzles and Extensions on Detonation Tube Performance," 38th AIAA/ASME/SAE/ASEE Joint Propulsion Conference and Exhibit, July 7–10, 2002, Indianapolis, IN, AIAA 02–3628.

[8]Bussing, T., "A Rotary Valve Multiple Pulse Detonation Engine (RVMPDE)," 31st AIAA/ASME/SAE/ASEE Joint Propulsion Conference and Exhibit, July 10–12, 1995, San Diego, CA, AIAA 95–2577.

[9]Aarnio, M. J., Hinkey, J. B., and Bussing, T. R. A., "Multiple Cycle Detonation Experiments During the Development of a Pulse Detonation Engine," 32nd AIAA/ASME/SAE/ASEE Joint Propulsion Conference, July 1–3, 1996, Lake Buena Vista, FL, AIAA 96-3263.

[10]McManus, K., Furlong, E., Leyva, I., and Sanderson, S., "MEMS Based Pulse Detonation Engine for Small Scale Propulsion Applications," 37th AIAA/ASME/SAE/ASEE Joint Propulsion Conference and Exhibit, July 8–11, 2001, Salt Lake City, UT, AIAA 2001–3469.

[11]Schauer, F., Stutrud, J., and Bradley, R., "Detonation Initiation Studies and Performance Results for Pulsed Detonation Engines," 39th AIAA Aerospace Sciences Meeting and Exhibit, January 8–11, 2001, Reno, NV, AIAA 2001-1129.

[12]Wintenberger, E., Austin, J., Cooper, M., Jackson, S., and Shepherd, J. E., "An Analytical Model for the Impulse of a Single-Cycle Pulse Detonation Engine," *Journal of Propulsion and Power*, Vol. 19, No. 1, 2003, pp. 22–38.

[13]Kuluva, N. M. and Hosack, G. A., "Supersonic Nozzle Discharge Coefficients at Low Reynolds Numbers," *AIAA Journal*, Vol. 9, No. 9, 1971, pp. 1876–1879.

[14]Kayser, J. C. and Shambaugh, R. L., "Discharge Coefficients for Compressible Flow Through Small-Diameter Orifices and Convergent Nozzles," *Chemical Engineering Science*, Vol. 46, No. 7, 1991, pp. 1697–1711.

[15]Gan, G. and Riffat, S. B., "Pressure Loss Characteristics of Orifice and Perforated Plates," *Experimental Thermal and Fluid Science*, Vol. 14, 1997, pp. 160–165.

[16]P. A. Kolodzie, J. and Winkle, M. V., "Discharge Coefficients Through Perforated Plates," *American Institute of Chemical Engineering Journal*, Vol. 3, No. 3, 1957, pp. 305–312.